



HAL
open science

Controlled switching of Néel caps in flux-closure magnetic dots

Fabien Cheynis, Aurélien Masseboeuf, Olivier Fruchart, Nicolas Rougemaille, Jean-Christophe Toussaint, Rachid Belkhou, Pascale Bayle-Guillemaud, Alain Marty

► **To cite this version:**

Fabien Cheynis, Aurélien Masseboeuf, Olivier Fruchart, Nicolas Rougemaille, Jean-Christophe Toussaint, et al.. Controlled switching of Néel caps in flux-closure magnetic dots. 2008. hal-00200915v2

HAL Id: hal-00200915

<https://hal.science/hal-00200915v2>

Preprint submitted on 29 May 2008 (v2), last revised 5 Mar 2009 (v3)

HAL is a multi-disciplinary open access archive for the deposit and dissemination of scientific research documents, whether they are published or not. The documents may come from teaching and research institutions in France or abroad, or from public or private research centers.

L'archive ouverte pluridisciplinaire **HAL**, est destinée au dépôt et à la diffusion de documents scientifiques de niveau recherche, publiés ou non, émanant des établissements d'enseignement et de recherche français ou étrangers, des laboratoires publics ou privés.

Controlled switching of Néel caps in flux-closure magnetic dots

F. Cheynis,^{1,2} O. Fruchart,^{1,*} J. C. Toussaint,^{1,2} N. Rougemaille,¹ and R. Belkhou^{3,4}

¹*Institut NÉEL, CNRS & Université Joseph Fourier – BP166 – F-38042 Grenoble Cedex 9 – France*

²*Institut National Polytechnique de Grenoble – France*

³*Synchrotron SOLEIL, L’Orme des Merisiers Saint-Aubin – BP 48, F-91192 Gif-sur-Yvette Cedex, France*

⁴*ELETTRA, Sincrotrone Trieste, I-34012 Basovizza, Trieste, Italy*

(Dated: May 29, 2008)

It has been proposed that two bits could be stored in magnetic dots exhibiting a flux-closure state, one bit in the chirality, another one in the core of the magnetic vortex. We go one step further, and show numerically and experimentally that three bits can be stored in an elongated dot. In this case the binary vortex is replaced by a domain wall displaying an extra degree of freedom, beyond its up-or-down core: the direction of Néel caps existing at both surfaces. We demonstrate the controlled switching of Néel caps under a magnetic field, without affecting the other two degrees of freedom.

Data storage relies on the handling of two states, called bits or '0' and '1'. In magnetoelectronic devices bits are stored using two directions of magnetization in nanoscale bistable domains. In hard-disk drives these are written in granular continuous thin films, while in solid-state Magnetic Random Access Memories (MRAMs) bits rely on single-domain flat dots patterned with lithography[1]. While miniaturisation is the conventional way to fuel the continuous increase of device density, disruptive solution are also sought. For patterned dots, *e.g.* disk-shaped, it has been proposed that bits could be stored in dots displaying a flux-closure magnetic state[2, 3]. Let us illustrate this by considering a flat dot with a square base (this discussion also applies qualitatively to the more common case of a disk-shaped dot). In a flat dot the magnetization lies in-the-plane and curls to follow the edges and close the magnetic flux lines, which reduces the dipolar energy (Fig. 1a-b). The chirality of the curling can be clockwise or anticlockwise, which provides one degree of freedom[2], or bit in terms of storage. In the very center of the dot the magnetization points out-of-the-plane, in order to lift the divergence of the exchange energy that would otherwise occur owing to the curling of magnetization. This central region is called a magnetic vortex and has a diameter roughly equal to ten nanometers[4]. The vortex can equally point upwards or downwards, defining its polarity which provides the second degree of freedom[3]. This flux-closure state is called a *vortex state*, and thus contains two micromagnetic degrees of freedom: the chirality and the polarity of the vortex. The prospect of using the vortex state as a two-bits recording cell has triggered a fast-increasing number of studies concerning the manipulation of the two degrees of freedom. The chirality can be controlled during magnetic hysteresis by *e.g.* introducing some asymmetry in the shape of the dot[5]. The core polarity can be switched using an out-of-plane magnetic field (≈ 0.4 T) without affecting the vorticity[6]. Recently it was shown that this

value can be significantly lowered, down to 1 mT, by applying the field as nanosecond-time-scale in-plane burst. This value is perfectly relevant for devices[7, 8]. Thus the two degrees of freedom in a micromagnetic vortex state might be used as two independent bits for fast, low consumption and high density solid-state magnetic devices in the future.

In this Letter we report a novel magnetization switching process within the domain wall of sub-micron-sized dots. This fundamental investigation has been achieved combining high-resolution magnetic imaging and micromagnetic simulations. With respect to the studies mentioned above we consider a modified design based on an elongated dot. In the case of elongated dots the vortex is replaced by a Bloch domain wall. This wall displays an extra degree freedom beyond the up-or-down polarity of its core: the direction of magnetization in the so-called Néel caps found at both surfaces at the vertical of the wall. These are well-known features of Bloch walls in thin films, which occur to decrease the magnetostatic energy. We demonstrate that this third degree of freedom can be switched under the application of a magnetic field applied along the in-plane short axis of the dot, without affecting the other two degrees of freedom. Thus based on this new switching process three bits, *i.e.* implying eight independent micromagnetic states, could in principle be stored in a single magnetic dot.

The sample consists of epitaxial micron-sized self-assembled Fe(110) dots. These were fabricated using UHV pulsed-laser deposition on Al₂O₃(11 $\bar{2}$ 0) wafers buffered with a high-quality layer of W(110). The dots display atomically-smooth facets. The anisotropy of the surface energy of these facets results in the dot elongation parallel to the in-plane crystallographic direction [001]. Details can be found elsewhere[9]. The growth temperature (450 °C) and nominal thickness (10 nm) were chosen so that the average length, width and height of the dots are 1 μ m, 0.5 μ m and 0.1 μ m, respectively. The dots were capped *in situ* with 0.7 nm-thick Mo followed by a 2.5 nm-thick Au layer to prevent oxidation during the transfer in air between the growth chamber and the magnetic imaging setup.

*Olivier.Fruchart@grenoble.cnrs.fr

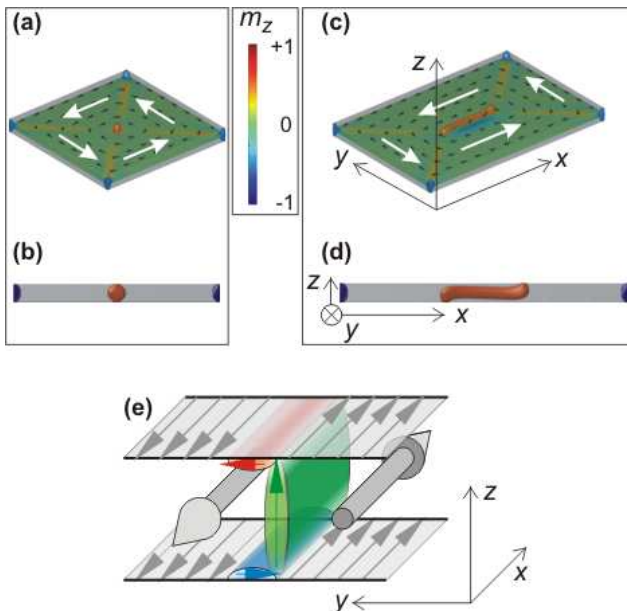


Fig. 1: 3D and cross section views of a so-called *vortex* state in a square magnetic dot (a and b, $500 \times 500 \times 50$ nm) and of a so-called *Landau* state in a rectangular magnetic dot (c and d, $700 \times 500 \times 50$ nm). Only volumes with normalized perpendicular magnetization $|m_z| > 0.5$ are displayed, which highlights the vortex and the domain wall. In (a-b) the map of m_z at mid-height is also shown, and the in-plane curling of magnetization is indicated by white arrows. (e) Schematic view of a domain wall of Bloch type, terminated by a Néel cap at each surface. The magnetization is opposite in the top and bottom Néel caps, and points along the $\pm y$ axes *i.e.* across the plane of the wall.

The high-resolution imaging experiments were performed on the Nanospectroscopy beamline (Elettra, Italy), using an Elmitec GmbH commercial LEEM/PEEM microscope (LEEM V). In the Low Energy Electron Microscopy (LEEM) mode[10], the topographical features of the studied objects is revealed with a lateral resolution better than 10 nm. In the X-ray Photo-Emission Electron Microscope (XPEEM) mode the microscope collects the total yield of secondary electrons emitted from the surface sample upon the absorption of the X-rays at a given element absorption edge. The spatial resolution of XPEEM is here 25 nm, with a maximum probing depth of 10 nm. We used XMCD-PEEM (X-Ray Magnetic Circular Dichroism) at the Fe L_3 edge ($h\nu = 707$ eV) where the difference of electron yield between opposite helicities of the X-rays is proportional to the dot product of the magnetization and the direction of the incoming circularly-polarized X-ray beam[11]. In our setup, the X-rays are incident on the sample at an angle of 16° from the surface, enabling to image mostly the in-plane component of magnetization.

The micromagnetic simulations were performed using GLFFT, a custom-developed code[12] based on a finite-differences scheme, *i.e.* the sample is discretized with

a regular array of prisms. The magnetization vector at each node is estimated as a second-order interpolation of the vector field between the cell and its nearest neighbors, so that the spatial variation of volume charges can be described linearly, not step-wise[13]. In practice the dots were divided into cells with uniform lateral and vertical size $\Delta_x = \Delta_y = 3.9$ nm and $\Delta_z = 3.1$ nm, respectively. Due to their large thickness and their full strain relaxation the dots are expected to be free from finite-size effects, and bulk magnetic properties of Fe at 300 K have been used accordingly: magneto-crystalline fourth-order anisotropy constant $K_1 = 4.8 \times 10^4$ J/m³, exchange energy $A = 2 \times 10^{-11}$ J/m and spontaneous magnetization $M_s = 1.73 \times 10^6$ A/m.

Fig. 1c-d illustrate the micromagnetic configuration of a dot with an elongated shape. Compared with dots with a high symmetry (Fig. 1a-b), the vortex is replaced by a domain wall (DW) aligned in the direction of the long axis of the dot. For thicknesses larger than a few tens of nanometers the magnetization in the DW remains in the plane of the DW and thus perpendicular to the surface of the dot. This arrangement is that of the conventional Bloch wall. However contrary to the text-book case where a translational invariance is assumed within the DW plane, here at both top and bottom interfaces the DW is terminated by an area with in-plane magnetization (Fig. 1e)[14, 15]. Such areas are called Néel caps (NCs). This name was given[16] because their magnetization distribution mimics that of a Néel wall, a type of DW with solely in-plane magnetization that occurs in ultrathin films[17]. NCs occur to reduce the dipolar energy at surfaces by closing the lines of magnetic flux above the DW. This overall arrangement is called an asymmetric Bloch wall. It has been described in detail in thin films[15] and more recently in dots[18, 19, 20, 21, 22]. It is worth to note that conceptually the asymmetric Bloch wall can be derived from a vortex without topological modifications, by shearing apart its top and bottom extremities (Fig. 1b,d). In the following we will call these extremities *surface vortices*. This way of building a Bloch wall implies a breaking of symmetry[19], *i.e.* the top vortex may be moved towards $+x$ or $-x$. As exemplified in the following, this symmetry breaking gives rise to two possible orientations of the top NC, which is thus an extra degree of freedom that does not exist in a symmetric dot in a vortex state. Notice that the chirality is still defined as the curl of the in-plane magnetization around the DW (*e.g.* anticlockwise in Fig. 1d), while the magnetization in the core of the DW may be either 'up' or 'down'. Therefore altogether such an elongated dot is described by three micromagnetic degrees of freedom.

At first, we report the results of micromagnetic simulations in elongated faceted Fe dots (Fig. 2). Their shape and size are those of the dots investigated experimentally. For a given in-plane chirality and a polarity of the Bloch wall, two degenerate ground states exist at zero external field, defined by the set of antiparallel NCs. We call these states after the y -orientation of the bottom and

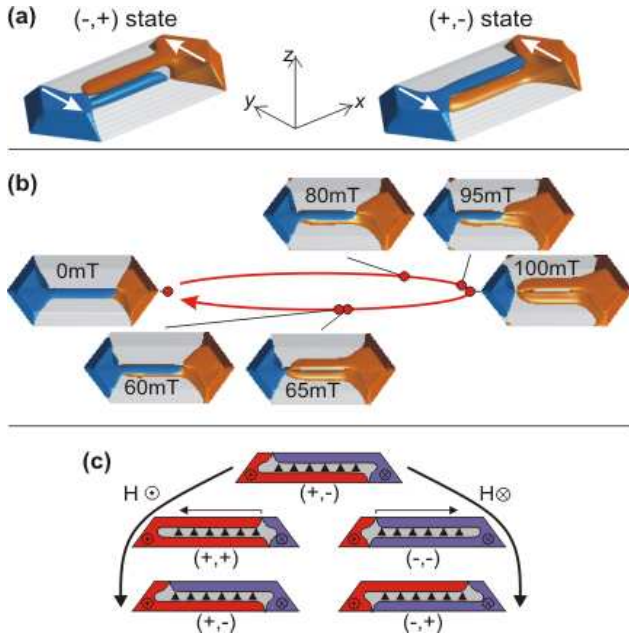


Fig. 2: (a) Micromagnetic simulation of the $(-, +)$ and $(+, -)$ states, as defined with respect to the orientation of the bottom and top Néel caps. Only volumes $|m_y| > 0.5$ are displayed, while positive and negative values appear red and blue, respectively. (b) Magnetization processes of Néel caps under $H_t > 0$ starting from a $(+, -)$ state (c) Schematic cross-sectional view of magnetization processes starting from a $(+, -)$ initial state: the final state is $(-, +)$ or $(+, -)$ depending on the sign of the applied field.

top NC respectively, *i.e.* $(-, +)$ and $(+, -)$ (Fig. 2a). Starting from a $(+, -)$ state at remanence, a transverse magnetic field H_t is applied (*i.e.* along y). Upon applying a positive H_t no significant change occurs up to 95mT (Fig. 2b). When H_t reaches 100mT the top surface vortex runs through the entire NC to finally settle essentially atop the bottom vortex. The two NCs are then parallel and aligned along the field direction [$(+, +)$ state]. This arrangement is called an *asymmetric Néel wall*, consistent with the findings in thin films that asymmetric Néel walls are favored against asymmetric Bloch walls under a transverse field[4, 23]. Upon decreasing H_t back to zero, no significant change occurs down to 60mT , where suddenly the surface vortex runs back to its initial position [$(+, -)$ state]. Upon decreasing the field towards negative values the top NC remains unaffected, while it is now the bottom surface vortex that runs through the dot, around $H_t = -100\text{mT}$ (Fig. 2c). Again, the system reaches a magnetic state with two parallel NCs aligned along the applied field, thus now $(-, -)$. Interestingly, when H_t is reduced back to zero it is again the top NC that switches back. This leaves a $(-, +)$ state at remanence, *i.e.* opposite to the initial state. The fact that it is always the top NC that switches back when the field is reduced towards zero might be related to the tilted facets (Fig. 3a-b), which break the symmetry between

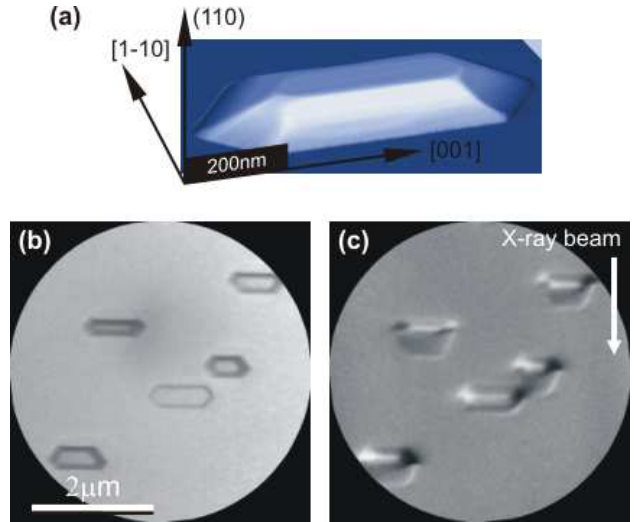


Fig. 3: (a) 3D view of a typical self-assembled epitaxial Fe(110) dot (Atomic force microscopy, true aspect ratios) . (b) LEEM (topography) and (c) XMCD-PEEM (magnetism) typical view of an ensemble of dots. After magnetization at -130mT the dots are in the $(-, +)$ state at remanence whatever their size, height or aspect ratio (see the white contrast over the Néel caps in c).

the top and bottom surfaces. To summarize, the micromagnetic simulations predict that the set of NCs can be switched by applying a magnetic field transverse to the dot, and that at remanence the top NC is antiparallel to the applied field (Fig. 2c). Notice that the $(+, +)$ and $(-, -)$ states are not stable at zero field, so that the set of NCs could be used to store one bit of information, not two.

The micromagnetic predictions were confirmed experimentally. Since no magnetic field can be applied while imaging, measurements were performed at remanence after *ex situ* application of a transverse magnetic field H_t with a given magnitude. Imaging several tens of dots at each stage reveals that starting from equiprobable $(-, +)$ and $(+, -)$ in the as-grown state, the occurrence of the $(+, -)$ state at remanence progressively increases to 95% for $H_t = +150\text{mT}$. The mean switching field is $H_{sw} = 120\text{mT}$ with a $\pm 10\text{mT}$ distribution. Similarly, 95% of $(-, +)$ states are found after application of $H_t = -150\text{mT}$. The value of the switching field ($H_{sw} = 120\text{mT}$) determined experimentally is in good agreement with the numerical simulations presented above (100mT).

Let us now come back to the other two degrees of freedom. The chirality is determined experimentally straightforwardly from the transverse component of closure domains at both end of the dots, which is imaged with XMCD-PEEM (Fig. 3c). Within the error bar related to the finite number of dots imaged, the occurrence of clockwise and anticlockwise chiralities remains similar for all applied magnetic fields. No cross-correlation

between the chirality and the state of the NCs could be evidenced either, still within the experimental error bars. The polarity of the DW core is not visible on the XMCD-PEEM images because first the probing depth is 10 nm only, second because owing to the grazing incidence of the X-ray in our setup we are mostly sensitive to in-plane magnetization. In principle the polarity of the DW core may be determined examining the details of the surface magnetization pattern[22]. However in most of the dots this could not be done reliably here because nearly half of the dot is invisible in XMCD-PEEM imaging, due to self-shadowing effects at the grazing incidence of X-rays used and the very small area of the top facet found on the average. Therefore we must rely on the simulations only, to notice that the core of the DW remains unaffected. Based on this combination of experiments and simulation we can safely claim that the NCs can be manipulated independently from the other two degrees of freedom.

To conclude we have demonstrated numerically and experimentally that the direction of magnetization of the NCs in elongated ferromagnetic dots can be switched back and forth using a transverse magnetic field. The switching affects neither the chirality of the in-plane domains nor the polarity of the core of the DW. This shows that there are three truly independent degrees of freedom in a single magnetic dot, whereas only two exist

in the now widely-studied vortex state found in high-symmetry dots. Whether this third degree of freedom could be exploited in multi-level logic or solid-state storage devices remains an open question. A prerequisite is to demonstrate that the NCs can be manipulated at high frequency and with a much smaller field magnitude than the 100 mT demonstrated here. This aim may not be non-realistic recalling that the field required to switch a vortex core has been reduced within a few years time from 0.4 T [6] to about 1 mT[7, 8, 24]. The use of spin-polarized current[25, 26], which promises an increased entanglement of magnetism and nanoelectronics in the future[27] and has been used recently to switch vortex cores[28], might also be a route.

Acknowledgments

We gratefully acknowledge discussions with A. Marty, P. Bayle-Guillemaud, L. Buda-Prejbeanu, A. Masseboeuf, A. Thiaville.

References

-
- ¹ C. Chappert, A. Fert, and F. Nguyen Van Dau, *Nature Mater.* **6**, 813 (2007).
 - ² J.-G. Zhu, Y. Zheng, and G. A. Prinz, *J. Appl. Phys.* **87**, 6668 (2000).
 - ³ N. Kikuchi, S. Okamoto, O. Kitakami, and Y. Shimada, *J. Appl. Phys.* **90**, 6548 (2001).
 - ⁴ A. Hubert and R. Schäfer, *Magnetic domains. The analysis of magnetic microstructures* (Springer, Berlin, 1999).
 - ⁵ A. S. Arrott, *Z. Metallkd.* **93**, 10 (2002).
 - ⁶ T. Okuno, K. Shigeto, T. Ono, K. Mibu, and T. Shinjo, *J. Magn. Magn. Mater.* **240**, 1 (2002).
 - ⁷ B. Van Waeyenberg, A. Puzic, H. Stoll, K. W. Chou, T. Tylliszczak, R. Hertel, M. Fähnle, H. Brückl, K. Rott, G. Reiss, I. Neudecker, D. Weiss, C. H. Back, and G. Schütz, *Nature* **444**, 461 (2006).
 - ⁸ Q. F. Xiao, J. Rudge, B. C. Choi, Y. K. Hong, and G. Donohoe, *Appl. Phys. Lett.* **89**, 262507 (2006).
 - ⁹ O. Fruchart, M. Eleoui, P.-O. Jubert, P. David, V. Santonacci, F. Cheynis, B. Borca, M. Hasegawa, and C. Meyer, *J. Phys.: Condens. Matter* **19**, 053001 (2007).
 - ¹⁰ E. Bauer, *Rep. Prog. Phys.* **57**, 895 (1994).
 - ¹¹ J. Stöhr, *J. Magn. Magn. Mater.* **200**, 470 (1999).
 - ¹² J. C. Toussaint, A. Marty, N. Vukadinovic, J. Ben Youssef, and M. Labrune, *Comput. Mater. Sci.* **24**, 175 (2002).
 - ¹³ O. Fruchart, J. C. Toussaint, P.-O. Jubert, W. Wernsdorfer, R. Hertel, J. Kirschner, and D. Mailly, *Phys. Rev. B* **70**, 172409 (2004), brief Report.
 - ¹⁴ A. Hubert, *Phys. Stat. Sol.* **32**, 519 (1969).
 - ¹⁵ A. E. LaBonte, *J. Appl. Phys.* **40**, 2450 (1969).
 - ¹⁶ S. Foss, R. Proksch, E. Dahlberg, B. Moskowitz, and B. Walsch, *Appl. Phys. Lett.* **69**, 3426 (1996).
 - ¹⁷ L. Néel, *C. R. Acad. Sci.* **241**, 533 (1955).
 - ¹⁸ A. S. Arrott, B. Heinrich, and A. Aharoni, *IEEE Trans. Magn.* **15**, 1228 (1979).
 - ¹⁹ A. S. Arrott and T. L. Templeton, *Physica A* **233**, 259 (1997).
 - ²⁰ R. Hertel and H. Kronmüller, *Phys. Rev. B* **60**, 7366 (1999).
 - ²¹ P. O. Jubert, J. C. Toussaint, O. Fruchart, C. Meyer, and Y. Samson, *Europhys. Lett.* **63**, 132 (2003).
 - ²² R. Hertel, O. Fruchart, S. Cherifi, P.-O. Jubert, S. Heun, A. Locatelli, and J. Kirschner, *Phys. Rev. B* **72**, 214409 (2005).
 - ²³ S. Middelhoek, *J. Appl. Phys.* **34**, 1054 (1963).
 - ²⁴ R. Hertel, S. Gliga, C. Schneider, and M. Fähnle, *Phys. Rev. Lett.* **98**, 117201 (2007).
 - ²⁵ L. Berger, *Phys. Rev. B* **54**, 9353 (1996).
 - ²⁶ J. C. Slonczewski, *J. Magn. Magn. Mater.* **159**, L1 (1996).
 - ²⁷ V. Cros, O. Boulle, J. Grollier, A. Hamzic, M. Muñoz, L. G. Pereira, and F. Petroff, *C. R. Physique* **6**, 956 (2005).
 - ²⁸ K. Yamada, S. Kasai, Y. Nakatani, K. Kobayashi, H. Kohno, A. Thiaville, and T. Ono, *Nature Mater.* **6**, 270 (2007).